A SMALL-SCALE TILTROTOR MODEL OPERATING IN DESCENDING FLIGHT

Anita I. Abrego and Mark D. Betzina
Army/NASA Rotorcraft Division
NASA Ames Research Center
Moffett Field, California

Kurtis R. Long
Aircraft Division
Naval Air Warfare Center
Patuxent River, Maryland

Abstract

A small-scale tiltrotor model was tested in the 7- by 10-Foot Wind Tunnel at NASA Ames Research Center with the goal of further investigating the aerodynamic environment of a tiltrotor operating in the Vortex Ring State (VRS). Test objectives were to obtain performance data of a 3-bladed tiltrotor model over a range of descent and sideslip conditions and to compare mean thrust results with a previously reported 2-bladed tiltrotor model investigation. Three sets of rotor blades, twisted and untwisted, were tested in a dual rotor configuration. Results of this investigation are presented, showing mean thrust reductions, a reduction in the effective lift curve slope and an increase in required collective pitch in the region of VRS. There was no consistent trend between the 2-bladed and 3-bladed untwisted blade sets or the two sets of twisted blades. Sideslip did not appear to significantly effect mean vehicle thrust.

Notation

C_T	Thrust coefficient, $T/2\rho(\Omega R)^2\pi R^2$
R	Rotor radius, ft
T	Total model thrust, lb
V	Air Velocity, ft/sec
V_{tip}	Rotor tip speed, ΩR, ft/sec
v_h	Equivalent hover induced velocity, $(T/4\rho\pi R^2)^{1/2}$
α	Shaft angle-of-attack, positive in descent, deg
α_G	Turntable angle, positive clockwise, deg
β	Model sideslip angle, deg
β_G	Sting pitch angle from horizontal, positive up, deg
$\theta_{0.75}$	Rotor collective pitch angle, deg
ρ	Air density, slugs/ft^3
Ω	Rotor rotational speed, rad/sec
RPM	Rotor rotational speed, rev/min
VRS	Vortex Ring State

Introduction

As a rotor's descent velocity in low-speed flight approaches the induced wake velocity in hover, a vortex ring is formed around the circumference of the rotor disk causing the flow to become very unsteady. This condition is known as the Vortex Ring State (VRS).

The aerodynamic characteristics of edgewise operating rotors in this VRS environment have been studied for many years. Reference 1 reports results from a wind tunnel test performed to study the empirical relation between the induced velocity, thrust and rate of vertical descent on four sets of rotor blades. Results showed force and moment fluctuations of the twisted blade set larger at the higher rates of descent than either the tapered or constant chord untwisted blades. In the 1960's, two propellers were tested at various rates and angles of descent, showing a reduction in rotor thrust, as well as thrust oscillations, in the region of VRS (Ref. 2). Thrust fluctuations on both single and tandem rotor configurations while operating in VRS, were reported in Refs. 3 and 4. Reference 5 reports results from a two-bladed model test with one set of untwisted blades and two sets of twisted blades operating in vertical descent. Results indicated thrust and torque fluctuations in the VRS. Results from the two twisted blade sets showed greater thrust reductions in VRS for the least twisted blade set.

More recently, the effects of descending flight on a tiltrotor were reported in Ref. 6. A single, 4-ft diameter, 3-bladed rotor, with twist and solidity similar to tiltrotors, was tested with an image plane to simulate the effects of a twin rotor tiltrotor system. Performance data were acquired over a range of descent conditions, with and without a

Report Documentation Page

1. REPORT DATE **SEP 2002**	2. REPORT TYPE	3. DATES COVERED **00-00-2002 to 00-00-2002**
4. TITLE AND SUBTITLE **A Small-Scale Tiltrotor Model Operating in Descending Flight**		5a. CONTRACT NUMBER
		5b. GRANT NUMBER
		5c. PROGRAM ELEMENT NUMBER
6. AUTHOR(S)		5d. PROJECT NUMBER
		5e. TASK NUMBER
		5f. WORK UNIT NUMBER
7. PERFORMING ORGANIZATION NAME(S) AND ADDRESS(ES) **US Army Aviation and Missile Command,Army/NASA Rotorcraft Division,Army Aeroflightdynamics Directorate (AMRDEC),Moffett Field,CA,94035**		8. PERFORMING ORGANIZATION REPORT NUMBER
9. SPONSORING/MONITORING AGENCY NAME(S) AND ADDRESS(ES)		10. SPONSOR/MONITOR'S ACRONYM(S)
		11. SPONSOR/MONITOR'S REPORT NUMBER(S)

12. DISTRIBUTION/AVAILABILITY STATEMENT
Approved for public release; distribution unlimited

13. SUPPLEMENTARY NOTES

14. ABSTRACT
see report

15. SUBJECT TERMS

16. SECURITY CLASSIFICATION OF:			17. LIMITATION OF ABSTRACT	18. NUMBER OF PAGES	19a. NAME OF RESPONSIBLE PERSON
a. REPORT **unclassified**	b. ABSTRACT **unclassified**	c. THIS PAGE **unclassified**	**Same as Report (SAR)**	**8**	

wing.   Mean rotor thrust reductions, thrust fluctuations, and an effective reduction in the rotor's lift curve slope were shown in VRS. Additionally, results indicated the need to acquire data with a two-rotor model and the need to investigate the suitability of using a single rotor with image plane apparatus to simulate the two-rotor flow field of a tiltrotor.   As a result, a small-scale tiltrotor model with 2-bladed, untwisted, teetering rotors was tested at various angles of descent and sideslip (Ref. 7). Dual-rotor, single-rotor with image plane, and isolated-rotor model configuration results were reported, each showing mean rotor thrust reductions in VRS. Results suggested the single-rotor with image plane model configuration might not properly capture the aerodynamic nature of a dual-rotor vehicle and recommended additional testing with a dual rotor model better representing the physical characteristics of a tiltrotor aircraft and the rotor system in particular.

Analytical results reported in Ref. 8 for both single dual rotor configurations indicated the onset and development of VRS is influenced by rotor configuration, such as blade twist, as well as rotor operating conditions.   Reference 9 reports experimental and theoretical results for the development of model rotor aerodynamics for steep descents. Dauphin 6075 flight test results were used to analyze the flight dynamics within the VRS and a comparison with the model developed during theoretical investigations was shown. The VRS area identification and the induced velocity measurements in vertical descent were shown. Experimental results revealed an increase in collective pitch did not permit the helicopter to leave the VRS regime and further collective pitch increases did not amplify the VRS effects. Increasing the forward velocity of the aircraft appeared to be the best way to quickly depart from VRS.

This paper presents the results of a study performed by NASA Ames Research Center and the U.S. Navy. In October 2001, a wind tunnel experiment was completed with the objective of further investigating the aerodynamic environment of a tiltrotor operating in helicopter mode over a range of descent and sideslip conditions.   A specific objective was to compare the mean vehicle thrust of a 3-bladed tiltrotor model operating in VRS with the previously tested 2-bladed model configuration reported in Ref. 7. Three sets of rotor blades were tested. These will be identified throughout the paper as untwisted, twisted-large-chord, and twisted-small-chord.

Test Description

Installation

Figure 1 shows the small-scale, 3-bladed tiltrotor model in the 7- by 10-Foot Wind Tunnel, at 90-deg descent angle or vertical descent. To minimize wall effects, the model was located at the center of the test section. The model was mounted onto a horizontal extension arm in a sideward orientation, equivalent to a 90-deg roll. Changes in model shaft angle-of-attack were provided by the wind tunnel turntable.   Sideslip angle, relative to the model longitudinal centerline, was achieved by manually rotating the extension arm upward about a horizontal axis, and is shown in Fig. 2 from the upwind side of the model.   The pitch axis, or turntable axis, did not yaw with the model in sideslip, therefore shaft angle-of-attack and sideslip angle for the model were computed from the following equations using the geometric pitch (α_G) and yaw (β_G) angles.

$$\alpha = \tan^{-1}(\tan\alpha_G/\cos\beta_G) \qquad (1)$$
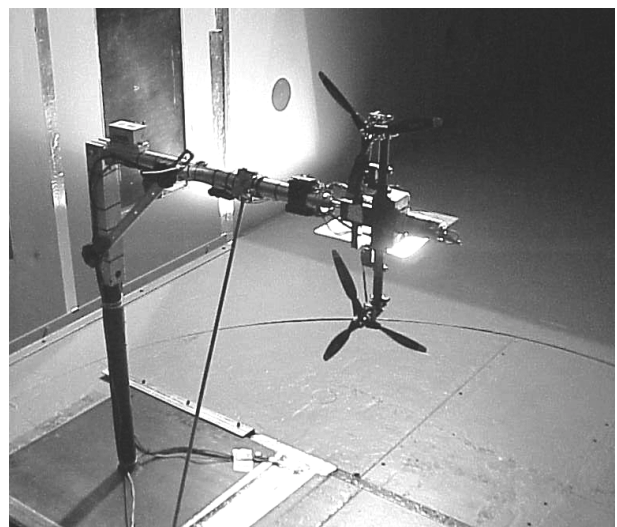
$$\beta = \sin^{-1}(\cos\alpha_G\sin\beta_G) \qquad (2)$$

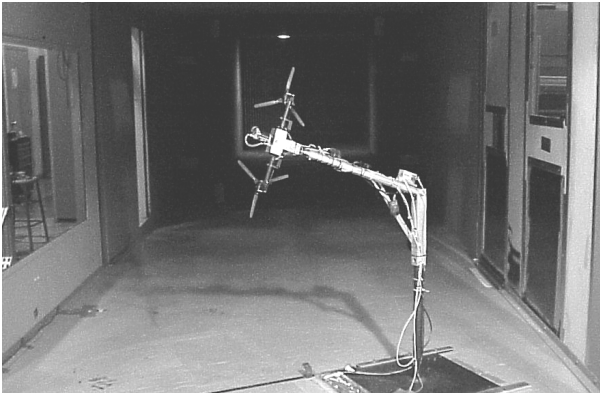**Fig. 1. Tiltrotor Descent Aerodynamics test in the Ames 7- by 10- Foot Wind Tunnel.**

Fig. 2. Tiltrotor model with sideslip.

Fig. 3. From top to bottom, 3-bladed model, twisted-small-chord, twisted-large-chord, untwisted blades and 2-bladed model untwisted blade from Ref. 7.

Model

Off-the-shelf radio-controlled (R/C) model helicopter parts were used to construct the 2-bladed tiltrotor model reported in Ref. 7. This model was reconfigured into a 3-bladed tiltrotor model. The model nacelle angle was fixed at 90 deg (i.e. helicopter mode) and the blades rotated with outboard advancing blades. The three different rotor blades tested during the 3-bladed test and the one rotor blade from 2-bladed test are shown in Fig. 3. The 2-bladed untwisted, 3-bladed untwisted, and the twisted-large-chord blade sets were purchased from a R/C parts supplier. The twisted-small-chord blade set was locally manufactured. Model and blade parameters are provided in Table 1, where 2B and 3B represent the 2-bladed and 3-bladed model configurations, respectively. Twist is defined as the twist at the blade tip with respect to the rotor shaft.

Commercially available hobbyist radio-control transmitter, receiver, speed control, and rpm governor units were used to remotely command rotor rpm and collective pitch. The rotors were driven by a single 700W brushed electric motor.

Test Conditions

Performance data were acquired over the range of test conditions shown in Table 2. Rotor speed was held constant at 5000 rpm and blade collective pitch values were chosen to represent full-scale thrust conditions. The variable test parameters included advance ratio (V/V_{tip}), collective blade pitch (θ), model shaft angle-of-attack (α), and sideslip angle (β). There was no measure of blade flapping; therefore descent angle is used throughout this paper when referring to shaft angle-of-attack. Descent angle was varied from 0 to 90 deg, in 5-deg increments, where a descent angle of 0 deg represented edgewise flight and a

Table 1. Model and blade parameters.

Parameter	2B Untwisted	3B Untwisted	3B Twisted Large chord	3B Twisted Small chord
Diameter	11.13 in	12.38 in	11.38 in	11.36 in
Average Chord	1.13 in	1.19 in	0.75 in	0.55 in
Twist	0 deg	0 deg	55 deg	46 deg
Thrust weighted solidity	0.127	0.183	0.126	0.093
Lock number	0.183	0.226	0.108	0.102
Root cutout	0.30R	0.24R	0.26R	0.26R
Rotor separation distance	2.55R	2.36R	2.57R	2.56R

Table 2. Test conditions.

Parameter	Value
RPM (rev/min)	5000
V/V_{tip}	0 to 0.12
$\theta_{0.75}$ (deg)	0 to 12
α_G (deg)	0 to 90 (5-deg increments)
β_G (deg)	0, 10

90-deg descent angle represented vertical descent. Descent angle sweeps for the 3-bladed untwisted and twisted-large-chord blade sets were completed at collective pitch angles ranging from 9 to 12 deg and advance ratios ranging from 0.06 to 0.10. The 3-bladed twisted-small-chord blades were tested at 12-deg collective pitch for advance ratios ranging from 0.06 to 0.12. Collective pitch sweeps were completed for each blade set in hover and for the 3-bladed untwisted blade set at 0.08 advance ratio for the full range of descent angles. Advance ratio sweeps were performed, with the twisted-small-chord blades, while maintaining a constant thrust coefficient and at constant collective pitch. A limited amount of data was acquired at 10-deg sideslip with the 3-bladed, twisted-small-chord blades.

Data Acquisition and Instrumentation

A 6-component internal balance measured model forces and moments. Model balance data were low-pass filtered at 100 Hz and acquired at 1024 samples per second per channel. Data were recorded at each test condition for an 8-second duration, producing time history records of 8192 samples for each record. Time history records were averaged to produce mean data. Mean thrust was used to calculate the vehicle thrust coefficient. A propeller anemometer, with a range of 1 to 130 ft/sec, was installed upstream of the model to measure air velocity in the wind tunnel test section.

Results

The effects of VRS on mean vehicle thrust will be shown for each of the 3-bladed model blade sets. For comparison, mean vehicle thrust results of the 2-bladed model (Ref. 7) will be shown. Twisted versus untwisted blade sets and 2-bladed versus 3-bladed untwisted blade set results will be discussed. The effective lift curve slope, the collective pitch required to maintain constant thrust in vertical descent, and the effect of vertical descent rate on mean vehicle thrust at constant collective pitch will be shown. The effects of sideslip angle will also be presented.
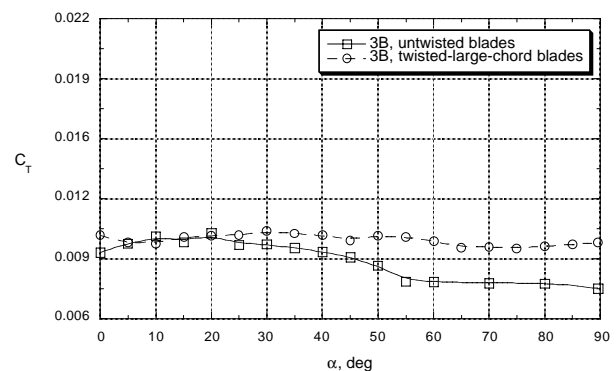
Mean Vehicle Thrust

Using Refs. 6 and 7 as a guide, descent angle sweeps were focussed on advance ratios ranging from 0.06 to 0.12 and collective pitch angles ranging from 9 to 12 deg. Figures 4 through 7 show the variation of mean vehicle thrust for constant advance ratio and collective pitch. The 2B and 3B legends indicate 2-bladed and 3-bladed data, respectively. For low descent angles, thrust

increases as a function of descent angle. Depending on advance ratio and collective pitch, the thrust begins to decrease starting at descent angles between 20 and 40 deg.
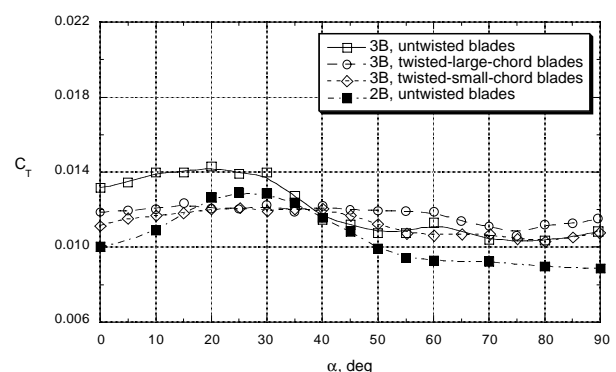
Figure 4 shows the mean vehicle thrust at 0.06 advance ratio. The 3-bladed, untwisted blades show a reduction in mean vehicle thrust starting at 20 to 25-deg descent angle for each collective blade pitch. The twisted-large-chord blades show a slight reduction in thrust beginning at 20-deg descent angle, for 9-deg collective pitch and very
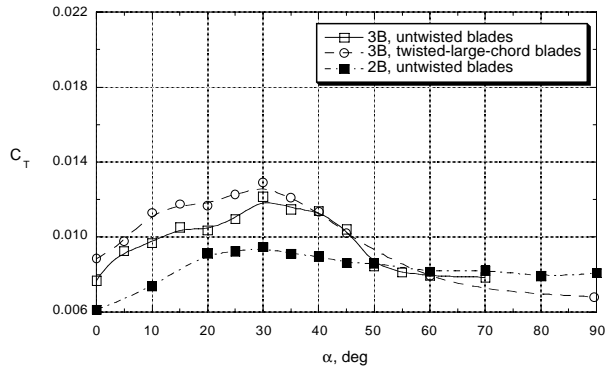

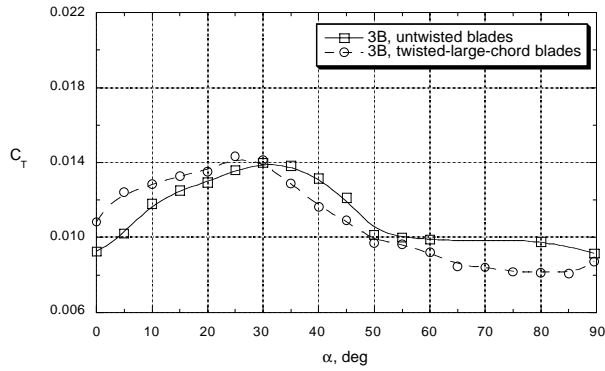**a) θ = 9 deg**
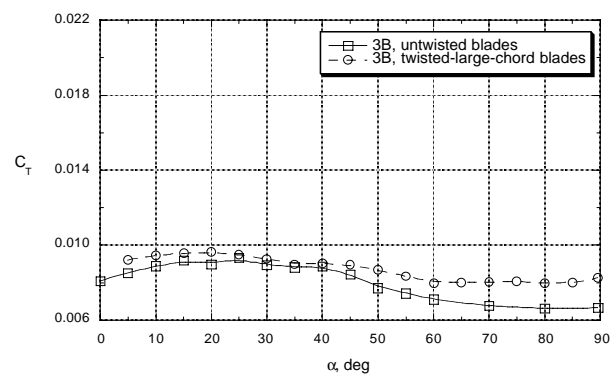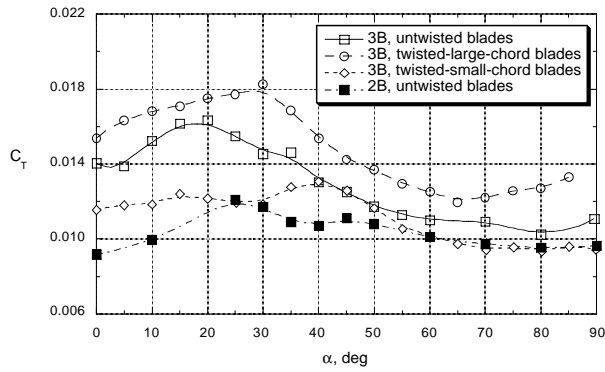

b) θ = 10.5 deg

c) θ = 12 deg

Fig. 4. Variation of mean vehicle thrust coefficient with descent angle, V/V_{tip} = 0.06

a) θ = 9 deg

b) θ = 10.5 deg

c) θ = 12 deg

Fig. 5. Variation of mean vehicle thrust coefficient with descent angle, $V/V_{tip} = 0.08$
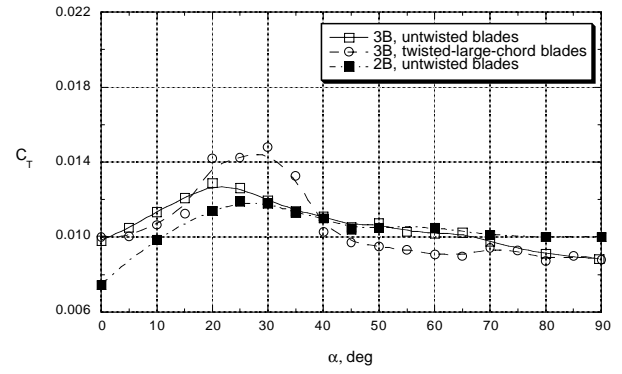

a) θ = 9 deg
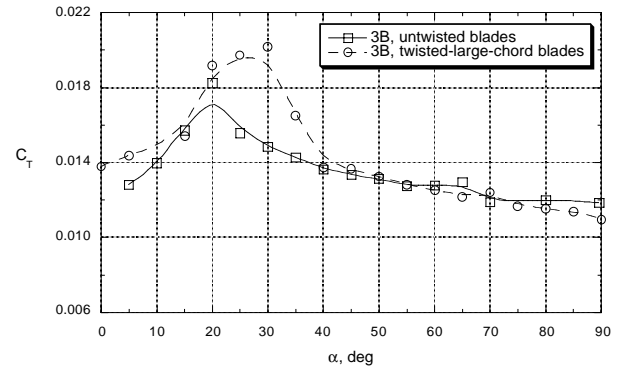

b) θ = 10.5 deg

c) θ = 12 deg

Fig. 6. Variation of mean vehicle thrust coefficient with descent angle, $V/V_{tip} = 0.10$

little variation in thrust at 10.5 and 12-deg collective pitch. The twisted-small-chord blades, at 12-deg collective pitch, show a thrust reduction beginning at 40-deg descent angle. The 2-bladed, untwisted blades, at 12-deg collective pitch, show a decrease in thrust at a descent angle of 30 deg. The 2 and 3-bladed untwisted rotors show a greater variation in thrust, when compared to the twisted blades, at 12-deg collective pitch.
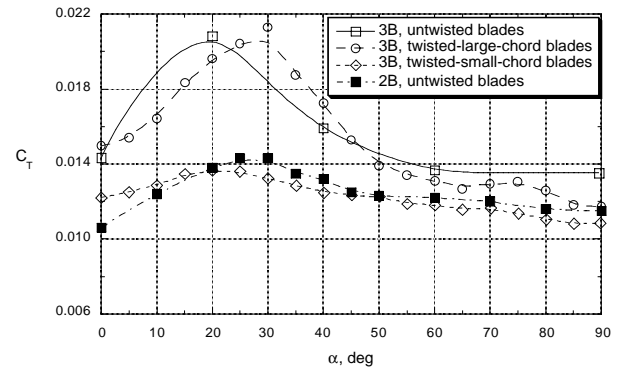
Mean vehicle thrust results at 0.08 advance ratio are shown in Fig. 5. At 9-deg collective pitch, the 2

and 3-bladed untwisted blade sets and the 3-bladed, twisted-large-chord blade set, show thrust reductions beginning at a descent angle of 30 deg. At 10.5-deg collective pitch, the 3-bladed, twisted-large-chord blades show an initial thrust reduction at 25-deg collective pitch and the 3-bladed, untwisted blades, show an initial thrust reduction at 30-deg collective pitch. At 12-deg collective pitch, the 3-bladed and 2-bladed, untwisted blades indicate an initial thrust reduction at 20 and 25-deg descent angle, respectively. The 3-bladed, twisted large and small chord blade sets

39.5

show a decrease in mean vehicle thrust at higher descent angles. Specifically, the thrust begins to decrease at a 30-deg descent angle for the twisted-large-chord blades and at a 40-deg descent angle for the twisted-small-chord blades. At 9 and 12-deg collective pitch the 2-bladed untwisted blade set has a shallow decrease in thrust with increasing descent angle, whereas the 3-bladed blade sets experience a greater reduction in thrust.

Figure 6 shows the mean vehicle thrust results at 0.10 advance ratio. The 3-bladed, untwisted blades show a decrease in mean vehicle thrust beginning at 20-deg descent angle, for each collective pitch. The 3-bladed, twisted-large-chord blades show a thrust reduction beginning at 30-deg descent angle for each collective pitch. At 12-deg collective pitch, the 3-bladed, twisted-small-chord blades show a reduction in mean vehicle thrust beginning at 20-deg descent angle. At 9 and 12-deg collective pitch, the 2-bladed, untwisted blades show an initial thrust reduction at 30-deg descent angle and again show a more shallow reduction in thrust when compared to the 3-bladed blade sets.

Figure 7 shows the mean vehicle thrust results for the 3-bladed, twisted large and small chord blades at 12-deg collective pitch. Both blade sets show an initial reduction in thrust at 25-deg descent angle.
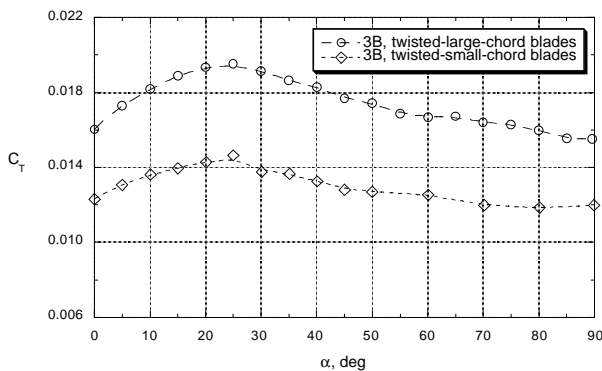

Fig. 7. Variation of mean vehicle thrust coefficient with descent angle, $\theta = 12$ deg, $V/V_{tip} = 0.12$.

The thrust reductions occurring between descent angles of 20 and 40 deg are consistent with general VRS characteristics. At 0.08 and 0.10 advance ratios, a larger variation in mean vehicle thrust is shown for the 3-bladed untwisted and twisted-large-chord blades. When comparing the 2 and 3-bladed untwisted blade sets, there was no

distinct difference in the initial onset of VRS induced thrust reductions. Although, the thrust reductions of 2-bladed untwisted blades were more shallow than the 3-bladed untwisted blades. As well, the two sets of twisted blades did not show a distinct difference in initial thrust reductions. The 3-bladed twisted-small-chord blades produced a smaller variation in thrust than the 3-bladed untwisted and twisted-large-chord blades.

Effective Lift Curve Slope

An additional method used to show the effects of VRS is to examine the effective lift curve slope (Ref. 6). Figure 8 shows the mean vehicle thrust coefficient versus collective pitch at constant descent angle at an advance ratio of 0.08 for the 3-bladed untwisted blade set. The slopes of all the curves are positive; indicating higher thrust is always achieved by increasing collective pitch. The slopes of the curves are lower for high descent angles, showing VRS causes a reduction in the vehicle's effective lift curve slope. The slope reduction occurs between descent angles of 20 and 25-deg and is consistent with the initial thrust reduction as seen in Fig. 5.
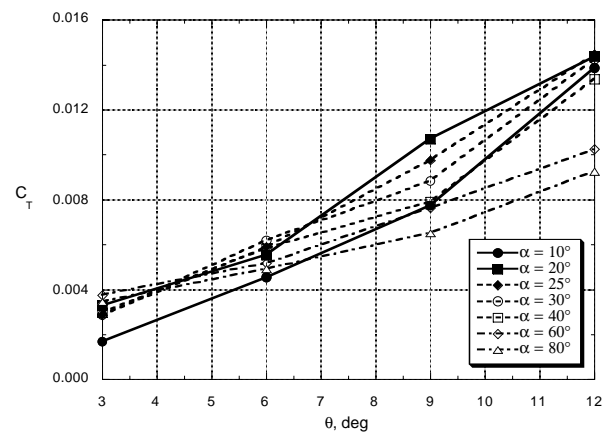

Fig. 8. Variation of thrust coefficient with collective pitch, no sideslip, 3-bladed, untwisted blades, $V/V_{tip} = 0.08$.

Effect of Vertical Descent Rate

Data were acquired with the 3-bladed, twisted-small-chord blades to investigate the effect of vertical descent rate on required collective pitch and mean vehicle thrust coefficient. Figure 9 shows the effect of vertical descent rate on the collective pitch required while maintaining a constant thrust of 0.13. For low descent rates, the collective pitch initially decreases with increasing advance ratio. At descent rates between 0.05 and 0.07 the collective pitch remains constant and from

0.07 to 0.11 descent rate a large increase in collective pitch is required to maintain a constant thrust. Above 0.12 descent rate the required collective pitch decreases rapidly with increasing descent rate. This increase in the required collective pitch between 0.07 and 0.11 is consistent with VRS related thrust reductions and the reduction in the rotor's effective lift curve slope. Additional advance ratio sweeps were performed to investigate the effect of vertical descent rate on mean vehicle thrust coefficient, while maintaining constant collective pitch (Fig. 10). At low descent rates, the thrust gradually increases with increasing advance ratio. The thrust begins to decrease with increasing advance ratios at conditions previously identified as regions of VRS. The 6-deg collective pitch curve shows a decrease in thrust between advance ratios of 0.05 and 0.08. Similarly, the 15-deg collective pitch curve shows a thrust reduction between 0.07 and 0.095 advance ratio. This decrease in thrust is consistent with VRS effects.
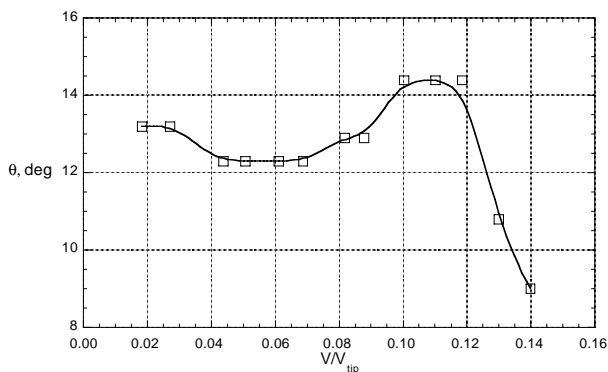

Fig. 9. Effect of vertical descent rate on required collective pitch, C_T = 0.013, α = 90°, 3-bladed, twisted-small-chord blades.

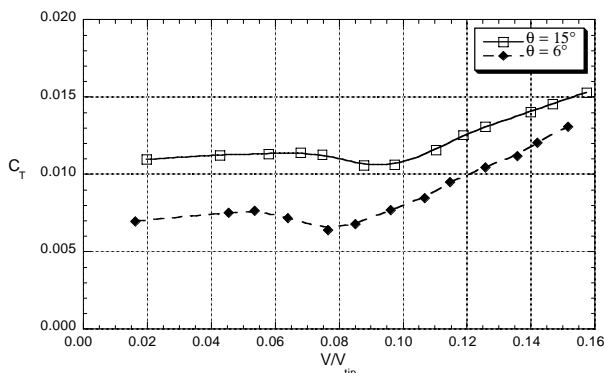**Fig. 10. Effect of vertical descent rate on mean vehicle thrust coefficient, constant collective pitch, α = 90°, 3-bladed, twisted-small-chord blades.**

Effect of Sideslip

The effects of sideslip angle on mean vehicle thrust was not evident in the 2-bladed, untwisted blade results reported in Ref. 7. Limited sideslip data were acquired for the 3-bladed, twisted-small-chord blades at 0 and 10-deg sideslip angle for a 0.10 advance ratio and 12-deg collective pitch. Figure 11 shows the variation of mean vehicle thrust versus descent angle. Again, mean vehicle thrust does not appear to be significantly affected by sideslip, although additional testing should be performed to further investigate the effect of larger sideslip angles.
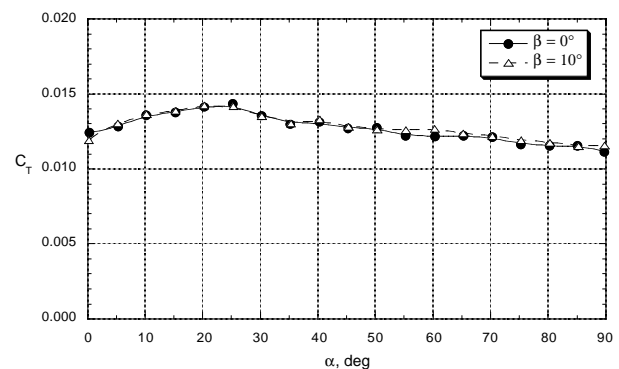

Fig. 11. Effect of sideslip angle on mean vehicle thrust coefficient with descent angle, 3-bladed, twisted-small-chord blades, V/V_{tip} = 0.10, θ = 12°.

Conclusions

A wind tunnel investigation was performed to study the effects of Vortex Ring State (VRS) on a small-scale 3-bladed tiltrotor model operating in descending flight. A reduction in mean vehicle thrust due to VRS is clearly shown for each blade set.

The specific findings from this investigation are:

1. Each rotor set tested resulted in significant VRS induced thrust reductions beginning between descent angles of 20 to 40 deg.

2. At 0.08 and 0.10 advance ratios, the 3-bladed untwisted and twisted-large-chord blades showed a larger variation mean vehicle thrust in the region of VRS.

3. There was no distinct difference in initial thrust reductions between any of the twisted and untwisted blade sets. Although, the 2-bladed, untwisted blades experienced a shallow reduction in thrust at larger descent angles. The 3-bladed,

twisted-small-chord blades showed a smaller variation in mean vehicle thrust.

4. A reduction in the lift-curve slope was evident at a descent angle above 20-deg.

5. Between vertical descent rates of 0.06 and 0.11, a large increase in collective pitch was required to maintain a constant thrust and a reduction in required collective was shown at descent rates above 0.11 advance ratio.

6. Sideslip did not appear to significantly effect mean vehicle thrust.

Although the small-scale model tested appeared to qualitatively capture the aerodynamic effects caused by VRS, additional research should be performed to further investigate the effects of model configuration, blade twist and scale. Further research should also be performed to investigate the effects of the fuselage and wings.

References

1. Castles, W. and Gray, R., "Empirical Relation Between Induced Velocity, Thrust, and Rate of Descent of a Helicopter Rotor as Determined by Wind-Tunnel Tests on Four Model Rotors," NACA TN 2474, October 1951.
2. Yaggy, P. and Mort, K., "Wind-Tunnel Tests of Two VTOL Propellers in Descent," NASA TN D-1766, March 1963.
3. Washizu, K., Azuma, A., Koo, J., and Oka, T., "Experiments on a Model Helicopter Rotor Operating in the Vortex Ring State," Journal of Aircraft, Vol. 3, No. 3, May-June 1966.
4. Washizu, K., Azuma, A., Koo, J., and Oka, T., "Experimental Study on the Unsteady Aerodynamics of a Tandem Rotor Operating in the Vortex Ring State," American Helicopter Society 22nd Annual Forum, Washington, DC, May 1966.
5. Xin, H. and Gao, Z., "An Experimental Investigation of Model Rotors Operating in Vertical Descent," 19th European Rotorcraft Forum, Cernobbio, Italy, September 1993.
6. Betzina, M., "Tiltrotor Descent Aerodynamics: A Small-Scale Experimental Investigation of Vortex Ring State," American Helicopter Society 57th Annual Forum, Washington, DC, May 2001.
7. Abrego, A. and Long, K., "A Wind Tunnel Investigation of a Small-Scale Tiltrotor Model in Descending Flight," American Helicopter Society Aerodynamics, Acoustics, and Test and Evaluation Technical Specialist Meeting, San Francisco, CA, January 2002.
8. Leishman, J. G., Bhagwat, M. J., Ananthan, S., "The Vortex Ring State as a Spatially and Temporally Developing Wake Instability," American Helicopter Society Aerodynamics, Acoustics, and Test and Evaluation Technical Specialist Meeting, San Francisco, CA, January 2002.
9. Taghizad, A., Jimenez, J., Binet, L., Heauzé, D., "Experimental and Theoretical Investigations to Develop a Model Rotor Aerodynamics Adapted to Steep Descents," American Helicopter Society 58th Annual Forum, Montréal, Canada, June 2002.